Available online at www.sciencedirect.com
SCIENCE DIRECT®
Journal of Magnetic Resonance 159 (2002) 1–12
JMR Journal of Magnetic Resonance
www.academicpress.com

T_1-relaxation of ^{129}Xe on metal single crystal surfaces—multilayer experiments on iridium and monolayer considerations

Dirk Stahl,[1] Wolfgang Mannstadt,[2] Peter Gerhard, Matthias Koch, and Heinz J. Jänsch*

Department of Physics and Material Sciences Center, Philipps University, Marburg D-35032, Germany

Received 19 February 2002; revised 20 August 2002

Abstract

The surface of a typical laboratory single crystal has about 10^{15} surface atoms or adsorption sites, respectively, and is thus far out of reach for conventional NMR experiments using thermal polarization. It should however be in reach for NMR of adsorbed laser polarized (hyperpolarized) ^{129}Xe, which is produced by spin transfer from optically pumped rubidium. With multilayer experiments of xenon adsorbed on an iridium surface we do not only demonstrate that monolayer sensitivity has been obtained, we also show that such surface experiments can be performed under ultra high vacuum conditions with the crystal being mounted in a typical surface analysis chamber on a manipulator with far-reaching sample heating and cooling abilities. With only four spectra summed up we present an NMR signal from at most 4×10^{14} atoms of ^{129}Xe, four layers of naturally abundant xenon, respectively. The fact that no monolayer signal has been measured so far is explained by a fast Korringa relaxation due to the Fermi contact interaction of the ^{129}Xe nuclei with the electrons of the metal substrate. T_1-relaxation times in the order of several ms have been calculated using all electron density functional theory for several metal substrates.

Keywords: NMR of single crystal metal surfaces; Xenon adsorption; Laser polarized resp. hyperpolarized ^{129}Xe; Korringa relaxation; Density functional theory

1. Introduction

The chemical shift range of physisorbed ^{129}Xe is about 400 ppm [1]. Therefore ^{129}Xe is a widely used NMR-probe for studying outer or inner surfaces of large surface area materials such as zeolites, clathrates, and dispersed catalysts [2,3]. Recently the use of highly nuclear polarized ^{129}Xe has also made feasible investigations of materials with a considerably lower surface area [4]. Such a high ^{129}Xe nuclear polarization, which is often called hyperpolarization, of up to 70% can be achieved by spin transfer from optically pumped rubidium [5,6]. This makes a signal enhancement of five orders of magnitude possible. Even single crystal surfaces, which have only about 5×10^{14} adsorption sites per cm^2, should be within reach for NMR of adsorbed hyperpolarized ^{129}Xe. Contrary to the large surface area samples, single crystal surfaces only offer a small number of different adsorption sites. The distribution of these sites can even be controlled over a certain range by choosing an appropriate crystal cut, by controlled precovering with other adsorbates etc., so that the identification of individual adsorption sites should be possible in an NMR-spectrum. For such "simple" systems it may even be possible that the experimental data can be compared to theoretical results from ab initio calculations. To study well controlled low area surfaces sample preparation, characterization and NMR measurement must take place under ultra high vacuum conditions (less than 10^{-9} mbar). Basic surface processes like adsorption, diffusion, and desorption may then be studied under well defined conditions. An apparatus has been

* Corresponding author. Fax: +6421-282-8993.
E-mail address: heinz.jaensch@physik.uni-marburg.de (H.J. Jänsch).
[1] Present address: Surface Science Center, Department of Chemistry, University of Pittsburgh, Pittsburgh, PA 15260, USA.
[2] Present address: Schott Glas, P.O. Box 2480, Mainz 55014, Germany.

1090-7807/02/$ - see front matter © 2002 Elsevier Science (USA). All rights reserved.
PII: S1090-7807(02)00006-X

designed to meet these experimental requirements. Parts of this apparatus have been described before [7]. A short description including improvements that have been made to enable the experiments described here is given in Section 2.1. Major problems arise from the fact that an NMR spectrometer is combined with conventional ultra high vacuum and surface analysis technology, which is not designed to work together with a sensitive radio frequency detector. In Section 2 we present pioneering multilayer experiments not only to demonstrate that NMR spectra can be obtained under such conditions but also that monolayer sensitivity has been reached with our apparatus.

A crucial point for the first attempts to reach monolayer (or even submonolayer) sensitivity for adsorbed ^{129}Xe is the question which kind of sample should be used. One could imagine pure metallic or nonmetallic crystals as well as crystals that have been precovered with various other adsorbates. Metal crystal surfaces are of particular interest, because shift measurements of ^{129}Xe for different adsorption sites could provide useful information for the interpretation of the ^{129}Xe spectra obtained from xenon adsorbed on various metal catalysts. In addition to that xenon adsorption has already been widely investigated on different metal single crystal surfaces by a variety of different surface analysis techniques such as thermal programmed desorption (TPD), photoelectron spectroscopy (UPS/XPS), scanning tunneling microscopy (STM), etc. [8]. By far fewer experiments have been performed on semiconductor surfaces, e.g. silicon(1 0 0) [9,10] and even less is known about xenon adsorption on insulator surfaces. This is mainly due to two reasons. On the one hand the character of the xenon binding to metal surfaces is of particular interest because it is in the transition regime between van der Waals and chemical interaction [11]. On the other hand xenon adsorbs on many metal surfaces in ultra high vacuum at temperatures of 80–100 K, so that liquid nitrogen cooling suffices for many experiments. In contrast to that, temperatures below 70 K are necessary for most nonmetal surfaces, so that liquid helium cooling is called for [12]. Last but not least a sample holder with good heating and cooling characteristics, that is small enough to fit between the pole shoes of the magnet and into the RF-coil of the NMR-probe, is much easier to be build for a metal crystal than for a nonmetal one. So there are several reasons why one should focus on metal crystals first. We have chosen an iridium crystal because of its low magnetic susceptibility of 3.8×10^{-5} (SI) [13] and because of its considerable inertness and its high melting point of 2683 K providing rather simple surface cleaning procedures.

However to perform NMR measurements of adsorbed hyperpolarized ^{129}Xe the T_1-relaxation on the surface has to be slow enough, so that the polarization does not decay considerably until the surface is covered and the NMR measurement is performed. For the present state of the apparatus this means that T_1 has to be at least a few seconds. In Section 3 we present theoretical considerations that deal with the important question of what T_1-relaxation time has to be expected and compare them to our first attempts to get a monolayer NMR-signal and other experimental results.

2. Multilayer experiments

Our experimental setup differs very much from conventional NMR spectrometers so that we first give a short description of our apparatus and the different modes of operation before we present the experimental results.

2.1. Apparatus

^{129}Xe is polarized by spin transfer from optically pumped rubidium. Therefore circularly polarized light from a titanium sapphire laser is radiated onto a glass cell that is filled with a mixture of about 5 mbar of xenon, 95 mbar of nitrogen, and 10^{-5} mbar of rubidium vapor, which is produced from a small droplet of rubidium by heating the glass cell to about 100 °C. A magnetic field of about 1 mT is applied to the cell to allow optical pumping. The mixture of polarized xenon and nitrogen is transferred to a liquid nitrogen cooled trap, which is situated between the pole shoes of the NMR magnet (Fig. 1), via a 6 m tube made of Per-Fluor-Alcoxy (PFA), a teflon derivative. No additional holding field is used in the transport. In the cold trap the xenon is frozen and the nitrogen is pumped away efficiently by the use of a small turbo molecular pump [6]. The crystal is situated in ultra high vacuum in a glass

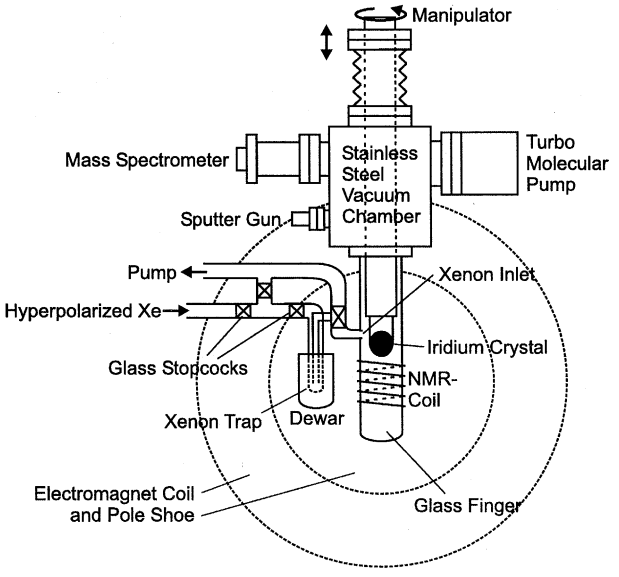

Fig. 1. Schematic drawing of the experimental setup.

finger that is mounted at the bottom of a stainless steel vacuum chamber and that is also situated between the pole shoes of the magnet. The trap and the glass finger are connected via a glass stopcock. The electromagnet is taken from a Varian XL100 spectrometer. It has a field of up to 2.4 T and an open slit of 33 mm between the pole shoes. The RF-coil of the NMR-probe is wound round the glass finger and is situated in the center of the pole shoes. The crystal is mounted at the end of a 1.6 m long manipulator, i.e., a hollow steel tube with a copper ending that can be filled with liquid nitrogen or liquid helium (see below) for cooling. The crystal is held in a loop made of a 0.5 mm molybdenum wire that can be heated by an electrical current of up to 50 A. A tungsten/rhenium thermocouple welded to the back of the crystal is used to determine the crystal temperature.[3] About 85 K was reached with pure liquid nitrogen cooling and about 75 K with the additional use of bubbling helium gas through the nitrogen[4] [14]. The vacuum chamber is equipped with a turbo molecular pump, a quadrupole mass spectrometer and a sputter gun for crystal cleaning. A more detailed description of the apparatus has already been published elsewhere [7].

Substantial changes in the setup have been made by the installation of liquid helium cooling of the sample. Liquid nitrogen cooling does not suffice to reach temperatures below 70 K, which are needed to adsorb xenon on a nonmetal surface or to grow xenon multilayers. Therefore a liquid helium cooling system has been added to the apparatus. Liquid helium is lead to the bottom of the manipulator through the vacuum insulated inner capillary of a double wall steel tube. The manipulator is closed and evacuated by a diaphragm pump so that the cold helium flows through the manipulator. Even though no further changes have been made with the manipulator, temperatures down to about 40 K have been reached at the crystal[5] at a liquid helium consumption of about 3 l/h.

[3] The heating wires and thermocouples act like antennas feeding radio frequency from the surrounding into the NMR-probe. Therefore several devices in the laboratory, including the turbo molecular pumps, have to be switched off during the NMR-measurement. With liquid helium cooling the vacuum is sustained by the cold manipulator, which acts as a cryo-pump. But even without liquid helium cooling there is enough time to carry out the NMR measurement while the rotors of the turbo molecular pumps are slowing down.

[4] The thermovoltage of the tungsten/rhenium thermocouple is already rather small at liquid nitrogen temperature so that the given temperatures have an uncertainty of about 10 K.

[5] Temperatures below 70 K could only be estimated from thermal programmed desorption measurements (TPD) of xenon, because at such low temperatures the thermovoltage of the tungsten/rhenium thermocouple is too small to be used for temperature measurement and because all known thermocouples with an appreciable thermovoltage become ferromagnetic at such low temperatures. In addition to that with liquid helium cooling the resistance of the molybdenum wire becomes so small that heating is only possible if the helium flow is reduced in addition to the electrical current.

Polarization measurement. Instead of the NMR-probe on the ultra high vacuum glass finger another home built NMR-probe for common sample tubes can be used to measure liquid or gaseous samples. To install this probe, the vacuum chamber has to be removed from the magnet. The laser polarized xenon gas can be taken from the polarization apparatus to this NMR-probe in a cylindrical glass cell, which is then inserted into the RF-coil. This way the xenon polarization was determined.

2.2. Surface covering modes

To obtain considerable NMR-signals of ^{129}Xe from an iridium crystal within the vacuum chamber xenon multilayers have been prepared in three different ways.

HT-fast-covering: high sample temperature and high xenon gas flow. Above 60 K xenon does not adsorb on xenon, so that it does not condense in ultra high vacuum. High xenon partial pressures in the mbar region are necessary to obtain bulk xenon at those temperatures. To grow multilayers on the liquid nitrogen cooled iridium crystal, such a partial pressure was achieved by filling the vacuum chamber with 1 mbar of nitrogen. This serves to hinder the xenon from flowing away from the crystal. One should notice that no clean metal surface could be prepared under these conditions, because the purity of the nitrogen gas was "only" 99.9990%. Usually about 1×10^{18} atoms of hyperpolarized naturally abundant xenon, 26.4% of which is ^{129}Xe, were stored in the liquid nitrogen cooled trap. A large xenon flow into the NMR region of the vacuum chamber was achieved by removing the liquid nitrogen filled dewar from the xenon filled cold trap after the stopcock separating the trap from the chamber had been opened. The xenon evaporates within 1–2 s. In this way a temporary xenon vapor pressure high enough to condense xenon was established in the vicinity of the crystal.

LT-slow-covering: low sample temperature and low xenon gas flow. To grow multilayers in ultra high vacuum the crystal was cooled with liquid helium. A crystal temperature of 45 K was estimated from xenon-TPD-measurements. To cover the iridium crystal slowly, the stopcock separating the trap from the vacuum chamber was opened while xenon was stored in the trap. The xenon vapor pressure in the trap of about 2×10^{-3} mbar at 77 K [15] leads to a mean xenon flux of 5×10^{14} atoms/s. Assuming a $\cos(\theta)$-distribution for the xenon flowing into the NMR region of the vacuum chamber and assuming a sticking coefficient of 1 for all cold surfaces [12], the fraction of the xenon that adsorbs on the crystal is estimated to be 15%, if the crystal is positioned directly in front of the xenon inlet. It has been taken into account that the cold manipulator and sample holder act as efficient pumps for xenon, so that nearly all atoms are "lost" that do not hit the crystal

directly.[6] One xenon layer[7] is therefore deposited on the crystal within about 7 s. After the crystal had been covered it was moved into the RF-coil which is situated about 2 cm below the xenon inlet.

LT-fast-covering: low sample temperature and high xenon gas flow. The second method of covering the surface under ultra high vacuum uses the fast expansion of the stored xenon described above. The liquid nitrogen filled dewar is quickly removed from the xenon trap, so that the whole load of 1×10^{18} xenon atoms is injected into the vacuum chamber within 1–2 s.

By comparing the signal strength of the spectra from the LT-fast-covered crystal with that from the LT-slow-covered crystal it is found that the fraction of xenon that adsorbs on the crystal does not depend on the mode of covering, if proper corrections are made for the T_1-relaxation in the trap and on the crystal (Section 2.3.2).

If the crystal is not covered directly in front of the xenon inlet but inside the RF-coil about 2 cm away from the inlet, the fraction of xenon reaching the crystal is much smaller, only about 2.6% of the xenon inserted into the vacuum chamber adsorbs on the crystal. This was found by comparing spectra at which the crystal has been covered in front of the xenon inlet with spectra at which the crystal has been covered inside the RF-coil.

2.3. Results

NMR of single crystal surfaces is performed on a quasi-two-dimensional sample with a metal crystal inside the RF-coil, which is connected to antenna-like heating wires and thermocouples, and with a stainless steel vacuum chamber inside the magnet coils. The following experiments have been performed to prove that NMR measurements can be performed though, i.e., that not only the crystal can be covered with polarized xenon but also that impedance matching of the NMR-probe and radio frequency detection of the NMR-signal are possible. Beyond that attempts have been made to approach monolayer sensitivity.

2.3.1. Experiments with N_2-background

Fig. 2 shows a sequence of ^{129}Xe-NMR spectra taken from the crystal while it was covered with the HT-fast-method, i.e., while xenon was flowing into the chamber. The resonance lines seen at 0 and 310 ppm belong to the well known resonances of gaseous and solid xenon

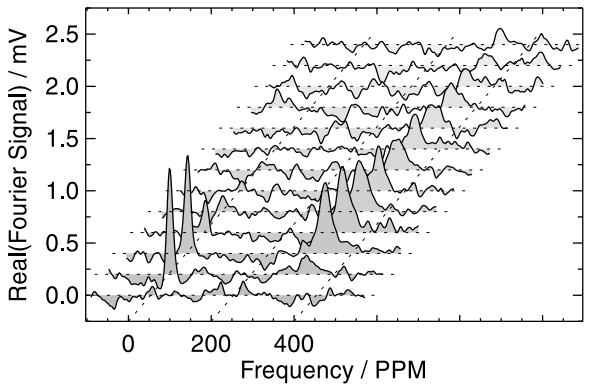

Fig. 2. ^{129}Xe-NMR spectra taken from a liquid nitrogen cooled Ir crystal at a rate of 1 spectrum/s while hyperpolarized Xe was inserted into the vacuum chamber, which was filled with a N_2-background of 1 mbar. The gas resonance is seen at 0 ppm and the solid resonance at 310 ppm.

[16,17]. The FWHM-linewidth of the solid resonance of about 430 Hz is considerably higher than the 350 Hz one would expect for a homogeneous solid. This and the nonGaussian shape of the solid resonance line are probably due to the magnetic susceptibility of the iridium crystal of 3.8×10^{-5} (SI) [13]. The gas resonance can only be seen because the nitrogen background gas prevents the xenon from immediately spreading over the whole vacuum chamber. When xenon condenses on the crystal the gas resonance disappears and the solid resonance appears. As the spectra have been taken with an approximate pulse angle of 45° only about one third of the polarization is destroyed by each pulse. Nevertheless the signal should vanish much faster than it actually does. There is obviously no large amount of polarized xenon in the gas phase inside the RF-coil anymore that could condense on the crystal, because otherwise the gas resonance should still be visible. This behaviour is still not well understood. Possibly polarized ^{129}Xe diffuses to the crystal from outside the RF-coil. Finally xenon evaporates from the crystal because the xenon partial pressure of the gas phase is too small to keep xenon solid when the xenon gas is spread over the whole vacuum chamber. Further analysis of this experiment is impossible because the amount of xenon that reaches the crystal through the nitrogen background is unknown.

However the spectra prove that highly polarized xenon reaches the crystal and condenses on it. Furthermore these experiments demonstrate that NMR spectra can be taken from a xenon film on a metal crystal inside the vacuum chamber.

2.3.2. Experiments in ultra high vacuum

LT-slow-covering. In Fig. 3 two spectra are shown which have been taken after the crystal had been covered for about 300 s (upper picture) and 60 s (lower picture) by the LT-slow-method. The amount of xenon adsorbed on the crystal, which is determined from the xenon flux onto

[6] Contrary to the liquid helium cooled manipulator the liquid nitrogen cooled manipulator (which is undoubtedly covered with water, CO, etc.) does not catch any xenon atoms because it is too warm to adsorb xenon. Therefore the liquid nitrogen cooled crystal is covered more quickly than the liquid helium cooled one.

[7] In all experiments that are presented here, xenon does not necessarily grow in layers. Therefore any given number of adsorbed layers only refers to the amount of xenon but not to the morphology of the xenon film.

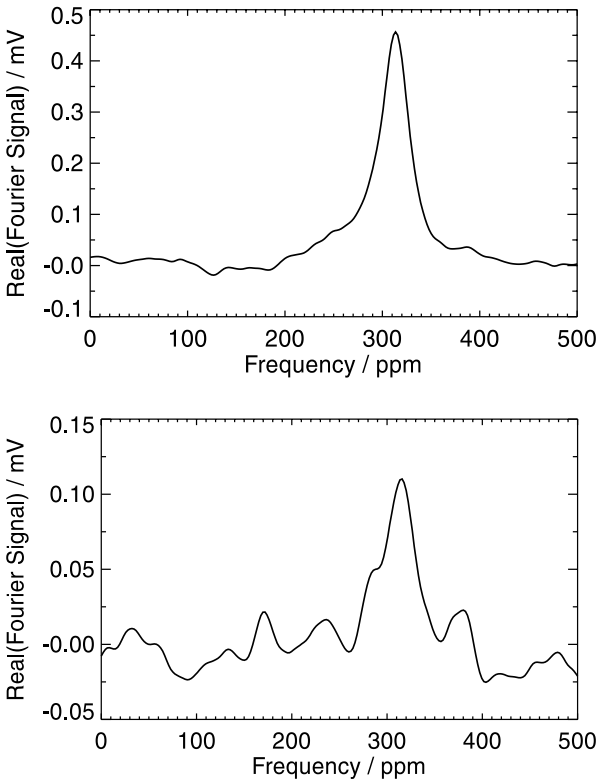

Fig. 3. ^{129}Xe NMR spectra from Xe films (natural abundance of isotopes) on a liquid helium cooled Ir crystal in ultra high vacuum made of about 2.3×10^{16} Xe atoms (upper picture) and 4.6×10^{15} Xe atoms, (lower picture), 45 and 9 layers of Xe, respectively. For the lower picture two spectra have been summed up to enhance the signal-to-noise ratio by a factor of $\sqrt{2}$. The ^{129}Xe content amounts to 11.5 and 2.5 monolayers, respectively.

the crystal, is about 2.3×10^{16} atoms, 45 layers, respectively, in the upper and 4.6×10^{15} atoms, 9 layers, respectively, in the lower picture. The signal-to-noise ratio, defined as the ratio between the height of the resonance line and the root mean square of the noise, in the upper picture is about 65, the one in the lower picture, for which two spectra have been summed up, is about 10. The difference in the signal-to-noise ratio per layer between the upper and the lower picture can be explained by fluctuations of the xenon flux, which affect the 60 s measurement more seriously than the 300 s one. Hence there are probably even less than 9 layers of xenon giving the signal-to-noise ratio of 10 in the lower picture. The ^{129}Xe content in this picture is at most 2.5 monolayers, thus demonstrating the high sensitivity achieved.

LT-fast-covering. The T_1-relaxation time of the solid xenon film on the crystal has been determined by varying the delay time between covering the crystal by the LT-fast-method and taking the NMR spectrum. T_1 is about 20 min, which is considerably shorter than the 410 min one would expect for solid xenon at 45 K [18–20]. This difference is too big to be explained by the uncertainty of the temperature. Since the xenon has a complicated "history" before it reaches the crystal, impurities have to be considered. Therefore relaxation due to paramagnetic impurities is a possible T_1-relaxation mechanism. The relaxation rate can be estimated from [21]

$$\frac{1}{T_1} = \frac{32\pi^3 \Delta_D^2}{15} S(S+1) \frac{N_S}{N_I} \frac{\gamma_S}{\gamma_I} \frac{T_{1,e}}{1 + (\omega_0 T_{1,e})^2}. \quad (1)$$

Δ_D is the dipolar linewidth and $T_{1,e}$ the relaxation time of the unpaired electron spins. Even if $T_{1,e} = \omega_0^{-1}$, so that the nuclear relaxation rate due to the impurities is at a maximum, the impurity density has to be $N_S/N_I \approx 10^{-6}$ in case of oxygen ($S = 1$), which is the only impurity one could imagine. However, the oxygen density in the xenon film on the crystal should rather be in the order of 10^{-8}. This results from the oxygen content in the trap of about 10^{10} atoms, which was determined by comparing the oxygen and xenon mass spectrometer signals when the stopcock between trap and vacuum chamber was opened. (To prevent the manipulator from "pumping" xenon, it was not cooled during this measurement.) The residual oxygen content in the chamber is neglectable at a base pressure of less than 10^{-9} mbar. Therefore relaxation due to paramagnetic impurities is probably not the reason for the short relaxation time.

Spin diffusion to the surface of the xenon film and a fast relaxation mechanism at the surface is another possible explanation. From a consideration similar to that in Abragam's book [22, Chapter IX, Section IIA] for relaxation due to paramagnetic impurities one gets $T_1^{-1} \approx 4D/d^2$ for spin diffusion to a quickly relaxing surface or interface. The film thickness of about 1000 atomic layers is $d \approx 1000 \times \sqrt{2/3}a$, with the atomic distance in solid xenon of $a = 4.4$ Å. The diffusion constant is estimated as $D \approx a^2 \pi \Delta_D / 30$, which gives $D \approx 600$ Å^2/s and $T_1 \approx 90$ min. This value is appreciably higher than the measured one, but as it is only a rough estimate this does not definitely rule out a relaxation mechanism by spin diffusion via the surface or the interface to the metal substrate. However we cannot imagine any relaxation mechanism at the xenon surface that would be fast enough at 45 K, because atomic diffusion should already be rather slow at that temperature. As xenon is adsorbed on a metal surface Korringa relaxation in the first two layers at the interface to the crystal must be considered, as it is done in Section 3.2. However from Table 1 it can be seen that this Korringa relaxation is expected to be accompanied by

Table 1
Results of the density functional calculations for the local density of states at the Fermi level at the ^{129}Xe nucleus (LDOS) and the resulting Korringa relaxation (T_1) and Knight shift (K) for xenon adsorbed on a platinum and a silver surface as well as on a platinum surface that has been precovered with either one layer of cesium or one layer of xenon

	Xe/Pt	Xe/Ag	Xe/Cs/Pt	Xe/Xe/Pt
LDOS(E_F) (eV^{-1} Å^{-3})	2.65	2.75	3.6	8.27×10^{-2}
T_1 (ms) at 100K	5.9	5.6	3.3	6.2×10^3
K (10^3 ppm)	2.4	2.5	3.2	7.5×10^{-2}

a Knight shift of about 3000 ppm in the first and about 70 ppm in the second xenon layer, which are both considerably bigger than the dipolar linewidth. Hence there should be no spin diffusion between the xenon bulk and the first two layers.

Our hypothesis to explain the short relaxation time of $T_1 \approx 20$ min is a structural difference between the quickly condensed xenon film on our crystal and the slowly condensed xenon solid in the experiments by Gatzke et al. [19] and Cates et al. [18], but we have no further idea of what this difference looks like. One argument for this hypothesis is that we find nearly the same relaxation time (22 min) for the xenon stored in the nitrogen cooled trap, which is also condensed very quickly, but should have a considerably different film thickness and which is not situated on a metal substrate, so that Korringa relaxation is ruled out.

Time resolved LT-fast-covering. To approach monolayer sensitivity an attempt has been made to obtain an NMR-signal from the surface layer of the xenon film adsorbed on the crystal. To get a great number of spectra with an appreciable part of surface atoms in each spectrum, time resolved measurements were performed with the crystal inside the RF-coil, while it was covered by the LT-fast method. ^{129}Xe spectra were taken at a rate of up to 12.5 spectra/s while xenon was evaporated. From the sequences of spectra it is found that the surface is covered at a rate of about 1.9×10^{16} atoms/s, 47 layers/s, respectively. Therefore during the 80 ms between each two spectra in the 12.5 spectra/s-measurement only 1.5×10^{15} new atoms, 4 layers, respectively, adsorb on the crystal. In the two upper pictures of Fig. 4 four such measurements have been summed up to double the signal-to-noise ratio. The appearance and the disappearance of the xenon bulk resonance line during the covering process can be seen at about 310 ppm. For the lowest picture all spectra from the upper pictures containing an appreciable xenon bulk signal have been summed up. From the sensitivity demonstrated here and in Section 2.3.1 one would have expected a second resonance line with a signal-to-noise ratio in the order of 10 from the xenon surface layer, which should have a considerably different chemical shift than the xenon bulk because of the reduced number of neighbouring xenon atoms. However no second resonance line could be found.

The high linewidth of the bulk resonance of about 1.5 kHz can be explained by the large amount of xenon that adsorbs on different parts of the crystal holder. Even though this xenon is situated outside the RF-coil, it contributes a broad background to the resonance line, because of its large amount.

The absence of a surface resonance can be explained by two possible reasons: first, the inhomogeneous structure of the surface layer could spread the chemical shifts of the various surface atoms, thus distributing the signal among several resonance lines each of which is too weak to be seen. In addition to that these lines could be broadened by atomic diffusion that is still not fast enough to cause motional narrowing. The other possible explanation is that spin diffusion distributes the polarization further into the bulk, thus lowering the polarization of the surface layer. From the estimated spin diffusion constant of $D \approx 600\,\text{Å}^2/\text{s}$ it is seen that the polarization diffuses about one atomic distance of 4.4 Å within the 80 ms between two spectra.

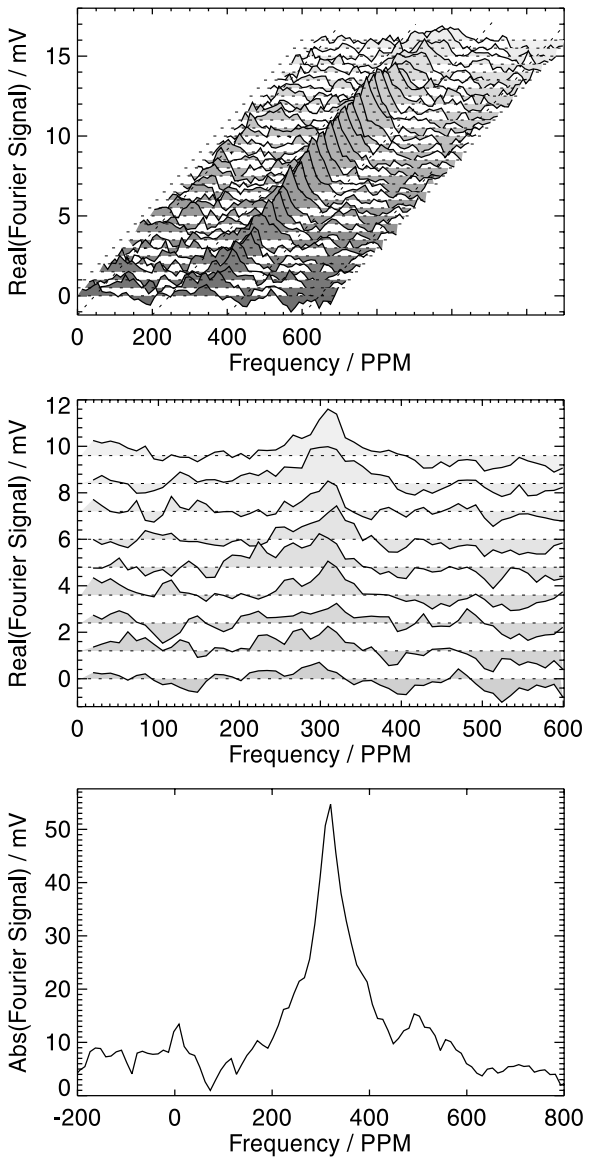

Fig. 4. ^{129}Xe-NMR spectra taken at a rate of 12.5 spectra/s while the liquid helium cooled Ir crystal was covered in ultra high vacuum at a rate of about 1.9×10^{16} Xe atoms/s. The second picture shows the first 9 spectra from the first one. The fourth spectrum is the first one that contains an appreciable ^{129}Xe NMR-signal originating from at most 1.5×10^{15} Xe atoms (3.9×10^{14} atoms ^{129}Xe), 4 layers of naturally abundant Xe, respectively. To double the signal-to-noise ratio 4 sequences of spectra have been summed up to obtain these pictures. The third picture shows the sum of all spectra in the upper pictures containing an appreciable NMR-signal.

From the density-functional-calculations presented in Section 3.2 it is expected that the first xenon layer on a metal surface relaxes totally within the 80 ms between two spectra, i.e., until the first spectrum is taken. However the second layer is expected to experience the metal, too. It should on the one hand relax within several seconds and should on the other hand differ from the bulk xenon appreciably in a Knight shift of about 70 ppm. Therefore one could hope to find the Knight-shifted resonance line of the second layer in the first spectra containing an appreciable NMR-signal in the upper pictures of Fig. 4. Unfortunately it is very difficult to find the related spectra in various measurements. Therefore it was not possible to extend the sum to more than four measurements. Thus the signal-to-noise-ratio could only be enhanced by a factor of two, which is not enough to identify any further resonance line apart from the bulk resonance. However if isotopically enriched xenon with a ^{129}Xe content of 70% is used in the future, the Knight-shifted second layer will probably be seen in this kind of experiment.

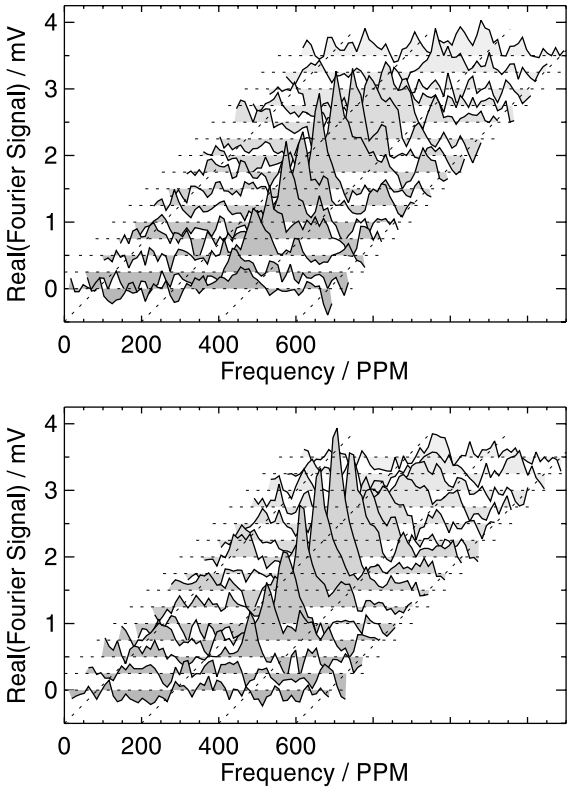

Fig. 5. ^{129}Xe-NMR spectra taken at rates of 6.25 (upper picture) and 3.125 spectra/s (lower picture) while the liquid helium cooled Ir crystal was covered in ultra high vacuum at a rate of about 1.9×10^{16} Xe atoms/s (natural abundance of isotopes). The first spectra containing appreciable NMR-signals, the second spectrum in the upper and the third spectrum in the lower picture, originate from at most 3.0×10^{15} Xe atoms, i.e., 7.8×10^{14} atoms of ^{129}Xe (upper picture) and at most 6.0×10^{15} Xe atoms, i.e., 1.6×10^{15} atoms of ^{129}Xe (lower picture), respectively 8 layers (upper picture) and 16 layers (lower picture) of Xe.

Nevertheless the first spectrum in the upper pictures of Fig. 4 containing an appreciable NMR-signal shows a resonance line from at most 1.5×10^{15} xenon atoms (4×10^{14} atoms ^{129}Xe), 4 layers of naturally abundant xenon, respectively, taken in ultra high vacuum from an iridium crystal.

The following spectra do not only contain the signal from the atoms adsorbed within the 80 ms after the previous pulse but also contributions from layers that have been adsorbed before, because the RF-pulse angle of about 45° only destroys about one third of the polarization. This pulse angle has been determined from the time dependence of the NMR-signal within sequences of spectra, which were taken with repetition rates of 3.125 and 6.25 spectra/s (Fig. 5).

2.3.3. Comparison with gas measurements

The signal strength found in the multilayer experiments that have been presented above agrees very well with the signal strength one would expect from xenon gas measurements. To compare the gas measurements with the multilayer experiments the gas signal strength is extrapolated to smaller amounts of xenon and wider resonance lines. For an optimally weighted signal (multiplication with its own envelope) the signal strength is proportional to the xenon amount, to the ^{129}Xe polarization and to the inverse of the linewidth [23] (This is absolutely correct only if the lines to be compared have the same shape, but even though they have not in our case the difference is neglected.). Therefore one can also get the amount of xenon adsorbed on the crystal by comparing the NMR signal from the crystal with that of the gaseous xenon. For the gaseous xenon the polarization and the amount of xenon have been determined rather accurately,[8] but the polarization on the surface cannot be measured directly. However the polarization produced is rather stable from batch to batch and was about 0.35 at that time and if one assumes that there is no loss in polarization through the process of covering the surface (which is justified by the result) the polarization on the surface was also 0.35. With this the fraction of the xenon inserted into the vacuum chamber that adsorbs on the crystal is about 12% which agrees very well with the 15% found from the geometrical considerations. Both numbers have uncertainties in the order of ±5%, the first because of the unknown ^{129}Xe polarization on the surface and the second because the distance between the crystal and the xenon inlet can be determined only at a certainty of about ±2 mm.

[8] Similar experiments to the gas measurements mentioned here have been published before [40]. Unfortunately a mistake has been made in these experiments when the amount of xenon was determined and therefore predictions have been made that were a factor of 7–8 too optimistic. If one corrects the amount of xenon the results agree with those given here.

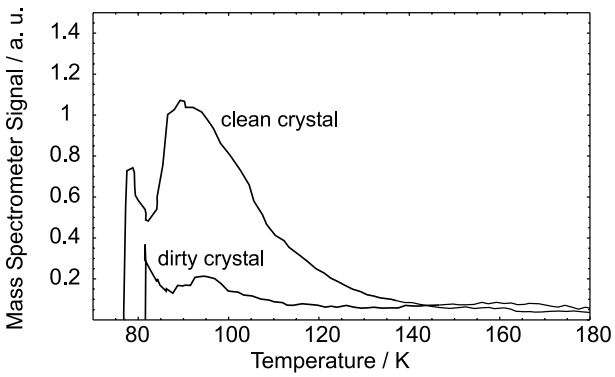

Fig. 6. Thermal desorption spectra of Xe from an Ir(1 1 1)-surface that has been cleaned and annealed by sputtering and heating to 1100 K and from a surface that has not been cleaned.

2.4. Monolayer sensitivity

With the experiments presented above it is demonstrated that ^{129}Xe-NMR experiments can be performed on a metal crystal in ultra high vacuum. It is also shown that for a linewidth in the order of the bulk linewidth of 300 Hz [16] and for a ^{129}Xe-polarization of 20–50% monolayer sensitivity is reached for natural abundant ^{129}Xe if only a few spectra are summed up.

However attempts to obtain a monolayer NMR-signal failed. These experiments have been performed with a liquid nitrogen cooled crystal in ultra high vacuum. The crystal temperature was about 80–90 K. At this temperature at most one monolayer of xenon adsorbs on the crystal. In Fig. 6 xenon thermal desorption spectra are shown to proof that xenon was really adsorbed on the crystal if the crystal had been cleaned and annealed by sputtering and heating prior to adsorption. At this temperature hardly any xenon adsorbs on the crystal if it is not cleaned. With a xenon flow of about 5×10^{14} atoms/s and a xenon pressure of about 1×10^{-5} mbar in the RF-coil the crystal is covered with a monolayer of xenon within 1–2 s. As monolayer sensitivity has been established by the multilayer experiments, a monolayer NMR-signal would have been expected for the sum of a few spectra if the ^{129}Xe polarization were in the order of 0.2–0.5 and the linewidth were in the order of the solid linewidth. Nevertheless no monolayer NMR-signal was found leading to the conclusion that either the ^{129}Xe surface resonance line is much broader than the solid linewidth or the ^{129}Xe polarization already decays considerably within the 1–2 s needed to cover the surface or even both.

3. Monolayer T_1-considerations

So far little is known about T_1 of adsorbed ^{129}Xe on metal surfaces. In bulk solid xenon in a high magnetic field (higher than 0.1 T) T_1 of ^{129}Xe is about half an hour at 100 K [18] and rises to more than 500 h at 4 K [19]. Unfortunately up to now most of the surface experiments have been performed at higher temperatures with considerably higher xenon gas pressures, so that the residence times on the surfaces have been much shorter than one second. Hence the relaxation times that have been measured this way are combinations of relaxation times in the gas phase, on the surface and during the adsorption and desorption processes. Long et al. [24] give for the adsorbed phase a T_1 of 20 s for ^{129}Xe on a polymer surface. On a graphite surface Neue has found a minimum T_1 of about 2 s at 90 K [25]. This "short" relaxation time is explained by the existence of paramagnetic centers on the surface.

At temperatures below 120 K Bifone et al. [3] observed a linear dependence of the ^{129}Xe-relaxation rates on temperature for xenon which was added to platinum clusters enclosed in NaY zeolite supercages. The relaxation rates were measured for the most shifted component of the spectrum. At 100 K a relaxation time of $T_1 = 14$ ms was found. This is interpreted as Korringa relaxation of xenon atoms adsorbed directly on the surfaces of the platinum clusters. However, the authors themselves stress that homogeneous metallic features cannot be attributed to the surfaces of clusters with an average diameter of 1 nm (about 55 atoms), which offer a variety of adsorption sites with different conduction electron densities. The surface structure of a single crystal is certainly very different from a cluster surface. The latter probably provides adsorption sites with much higher binding energies.

For ^{13}C-NMR of CO on platinum catalysts Korringa relaxation has been found to be the dominating relaxation mechanism, too, even at room temperature [26]. However, the relaxation time is about 0.6 s at 100 K, i.e., two orders of magnitude slower than that of ^{129}Xe on platinum clusters.

The only NMR experiments with adsorbates on single crystal surfaces so far have been performed with alkali adsorbates by the use of different alkali-specific NMR techniques that provide extremely high signal-to-noise ratios [27]. At a temperature of about 100 K T_1-relaxation times of 3–10 s have been found for ^{8}Li on a ruthenium surface [28]. It is not obvious that the weakly interacting (physisorbed) xenon should experience a faster Korringa relaxation than the strongly interacting (chemisorbed) species ^{13}CO and lithium.

3.1. Surface relaxation mechanisms

In the absence of paramagnetic centers only a few relaxation processes come into question for a fast T_1-relaxation that would explain that no monolayer signal could be measured so far (see Section 2.4): fluctuations of the dipole–dipole interaction between neighbouring xenon atoms, fluctuations of the anisotropic chemical

shift, both due to diffusion of the xenon atoms on the surface and Korringa relaxation due to the Fermi contact interaction of the xenon adsorbate nuclei with the conduction electrons of the substrate. The spin phonon interaction that dominates the relaxation in the bulk for temperatures below 120 K [19,20] leads to much longer relaxation times.

The relaxation due to adsorbate diffusion depends on the structure of the adsorbate layer and the diffusion processes in detail and is therefore difficult to be calculated. However a fair estimate for the dipolar relaxation can be obtained from [22, Chapter VIII, Section IIE]

$$\frac{1}{T_1} \approx n_N \theta(1-\theta) \frac{\mu_0^2}{(4\pi)^2} \frac{2}{5} \frac{\gamma^4 \hbar^2}{c^6} I(I+1) \times \left(\frac{\tau_c}{1+(\omega_0 \tau_c)^2} + 4 \frac{\tau_c}{1+(2\omega_0 \tau_c)^2} \right) \quad (2)$$

at which the coverage dependency of the atomic diffusion is taken into account by the factor $\theta(1-\theta)$ [29, 30]. For this estimate only the coupling among the ^{129}Xe-nuclei is taken into account, the coupling to the ^{131}Xe-nuclei, which is in the same order of magnitude, is neglected. With $n_N = 6$ nearest neighbours and an atomic distance of $c = 4.8$ Å in for example the commensurate close packed xenon layer on a platinum(1 1 1)-surface [31] and with a resonance frequency of 23.3 MHz this gives a minimum T_1 of about 50 min for a xenon coverage of $\theta = 0.5$. Therefore the dipole–dipole interaction should not lead to short relaxation times in the ms-range. A similar estimate can be obtained for the anisotropic chemical shift by [22, Chapter VIII, Section IIF]

$$\frac{1}{T_1} \approx n_N \theta(1-\theta) \frac{1}{15} (\omega_0 \sigma_a)^2 \frac{2\tau_c}{1+(\omega_0 \tau_c)^2}, \quad (3)$$

in which σ_a is the difference between the maximum and the minimum anisotropic shift due to the diffusion of a neighbouring xenon atom. This certainly depends on the orientation of the surface with respect to the magnetic field. If one assumes σ_a to be in the order of $1/12$ of the bulk (isotropic) chemical shift this gives a minimum T_1 of about 2 min, which is still rather long. Nevertheless one should keep in mind that this is based on an assumption for σ_a, on which T_1 depends quadratically. On the other hand these are the minimum relaxation times caused by diffusion, which appear for $\omega_0 \tau_c = 1$, respectively $\omega_0 \tau_c = 0.6$ for the dipolar interaction. The corresponding temperature can be found from the relation for two-dimensional diffusion, $a^2 = 4D\tau_c$ [30], at which $D = D_0 \exp(-E_D/k_B T)$ is the diffusion constant. For xenon on platinum(1 1 1) Meixner and George give a prefactor of $D_0 \approx 2.3 \times 10^{-4}$ cm^2/s and a diffusion barrier of $E_D/k_B \approx 625$ K [32]. With a Larmor frequency of 23.3 MHz the minimum relaxation time is found at about 80 K, which is right in the range where the unsuccessful monolayer experiments with liquid nitrogen cooling have been performed. However at 45 K, which was reached by liquid helium cooling, relaxation due to atomic diffusion should be much slower.

So far the difference between diffusional relaxation in two and in three dimensions has not been taken into account. However Korb et al. [33] have shown that the relaxation due to two-dimensional diffusion can be orders of magnitude faster than that in three-dimensional systems if the diffusion is restricted to a small area (and for very small magnetic fields even if the diffusion is not restricted). Nevertheless for high fields (Lamor frequencies in the kHz-region and higher) and without considerable spacial restrictions this two-dimensional theory gives relaxation times very similar to the rough estimate above and there is no reason to believe that the diffusion of xenon atoms on a single crystal surface is spacially restricted.

3.2. Korringa relaxation on metal surfaces

The relaxation processes discussed so far are not specific for any kind of surface whereas Korringa relaxation can only take place on metal surfaces.

On the one hand one would expect the Korringa relaxation of the weakly bound ^{129}Xe on metal single crystal surfaces to be slower than that of the strongly bound lithium, i.e., longer than a few seconds. On the other hand the results from Bifone et al. [3] suggest a much faster Korringa relaxation for adsorbed ^{129}Xe on metal surfaces in the order of milliseconds. The latter is supported by recent density functional calculations that also predict relaxation times in the order of only a few ms (Table 1). The relaxation time has been obtained from the local density of states at the xenon nucleus at the Fermi energy (LDOS) by [22]

$$\frac{1}{T_1} = \frac{4\pi}{9} \mu_0^2 \gamma_e^2 \gamma_I^2 \hbar^3 \mathrm{LDOS}^2(E_F) k_B T. \quad (4)$$

Often LDOS is written in the form $\mathrm{LDOS}(E_F) = \mathrm{DOS}(E_F) \cdot |\Psi(0)|^2$, i.e., the product of the density of states at the Fermi energy times the wave function squared at the nucleus ($r = 0$). From T_1 estimates of the Knight shift have been obtained by use of the Korringa relation [22]

$$T_1 K^2 = \frac{\hbar}{4\pi k_B T} \left(\frac{\gamma_e}{\gamma_I} \right). \quad (5)$$

The knowledge of the electronic structure reveals the LDOS and thus determines the T_1-time (Eq. (4)). State of the art calculations within the density functional theory (DFT) formalism were performed for a theoretical approach to the T_1 time. We employed the FLAPW (full potential linearized augmented plane waves) method [34, and references therein] implemented in the recently developed parallel version of the code

(P-FLAPW) [35, and references therein]. This code has the special design to handle both two-dimensional and three-dimensional systems, thus being very well suited of surface related problems. An accurate description of the wave functions near the nucleus is crucial for a reliable value for the LDOS. The FLAPW method is an all electron method with no shape approximation for the potential. This allows in particular the local description near the nucleus, in contrast to other methods like in pseudo-potential approach. The reliability of this type of calculation has been shown for ^{8}Li adsorbed on ruthenium(0 0 1), where the theoretical result of $T_1 = 6$ s [36] at 100 K compares favorably to an experimental value of 9 s [37].

For xenon adsorption the clean metal surface (platinum or silver) was modeled by a 5 layer slab. A monolayer coverage of xenon in the well known commensurate hexagonal $\sqrt{3} \times \sqrt{3}$-structure was calculated. Furthermore the influence of a monolayer cesium adsorbed on the platinum surface as well as a second layer of xenon was investigated. Fig. 7 shows for example the local electronic density of states at the xenon nucleus calculated for a platinum substrate. Even though only a very small part of the electronic density is found at the Fermi energy the amount suffices to cause a very short T_1-relaxation time of 6 ms. Further details of the calculations will be published separately by Mannstadt.

Here we want to compare the theoretical results for the Korringa relaxation on single crystal surfaces to the experimental results on metal clusters by Bifone et al. and to the fact that no monolayer signal could be measured on an iridium(1 1 1)-surface even though monolayer sensitivity had been established for the apparatus (see Section 2.4). Both experimental findings agree with the theoretical predictions, suggesting that the fast Korringa relaxation on the metal clusters is not due to the specific cluster structure but is a general feature of ^{129}Xe adsorbed on metal surfaces. This is probably based on the fact that xenon adsorption on metal surfaces is not pure physisorption, i.e., not a pure van der Waals interaction, but has an appreciable chemical part, which leads to charge transfer between the metal and the xenon atom. Such a charge transfer is known to be responsible for the 'visibility' of xenon in STM-pictures on metal surfaces [38] and has been explained by Wandelt and Gumhalter [39] with a broadening of the 6s-level of adsorbed xenon. Nevertheless it is astonishing that this charge transfer leads to a Korringa relaxation that is so much faster than that of the alkali metal atom lithium. The physical reason could be a concentration of the electron wave function at the xenon nucleus due to its high nuclear charge. This trend can be clearly seen in the hyperfine splittings of the free alkali atoms. It increases from a few hundred MHz for lithium to about 10 GHz for caesium, roughly a factor of 30. The splitting is proportional to $|\Psi(0)|^2$. This quantity also enters the Korringa relaxation but squared. Tentatively this leads to a three orders of magnitude difference in the relaxation rates between Li and Xe. Following this interpretation the high spin transfer rates in the optical pumping process, which enable the high nuclear polarization (and the current experiments), and the fast Korringa relaxation on metal surfaces stem from the same physical effect.

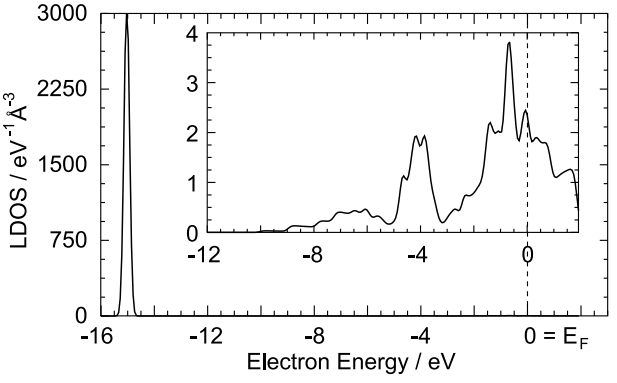

Fig. 7. Local density of states at the nucleus of a xenon atom adsorbed on a platinum surface, calculated by density functional theory with a local density approximation. Even though only a small part of the density is found at the Fermi energy the amount suffices to cause a strong Korringa relaxation with $T_1 = 6$ ms.

4. Conclusions

The multilayer experiments demonstrate that NMR experiments can be performed under ultra high vacuum conditions on a thin xenon film adsorbed on a metal crystal that is attached to a common sample manipulator for surface analysis. In spite of the stainless steel vacuum chamber inside the magnet coils, the flatness of the sample, the metal crystal in the RF-coil and the antenna-like heating wires and thermocouples the crystal is connected to, impedance matching of the NMR-probe and conventional radio frequency NMR-detection are still possible. Moreover it has been shown that monolayer sensitivity can be obtained for NMR of hyperpolarized ^{129}Xe on a typical laboratory single crystal with an area of less than 1 cm^2, provided neither the surface resonance is much wider than 1 kHz nor the T_1-relaxation time is much smaller than 1 s. Nevertheless we did not observe a surface resonance on the iridium(1 1 1)-surface. Together with the DFT-calculations for the local density of states this indicates a fast Korringa-relaxation, most likely in the order of several ms, for ^{129}Xe adsorbed on metal surfaces. This means that further attempts to obtain a monolayer signal should first be made with a nonmetal surface, e.g., silicon(1 0 0) or the modified, e.g., oxidized, surface of a metal crystal. Nevertheless metal surfaces are not totally out of reach

for ^{129}Xe-NMR even if the T_1-relaxation is thus fast. One could imagine continuous flow experiments at a higher temperature, at which the mean residence time of the xenon atoms on the surface is in the order of T_1, so that the polarization of the nuclei on the surface is always appreciably high. Our apparatus still does not provide the high xenon flux necessary for such experiments, but changes, i.e., a reconstructed xenon trap and liquid argon instead of liquid nitrogen cooling of the trap, are under way to obtain such a flux.

Acknowledgments

We would like to thank Dieter Fick for providing continuous support and inspiration and for many fruitful discussions. This work was supported by the Deutsche Forschungsgemeinschaft under various grants. The support received is gratefully acknowledged.

References

[1] T. Pietraß, H.C. Gaede, Optically polarized ^{129}Xe in NMR spectroscopy, Adv. Mater. 7 (1995) 826–838.

[2] C. Dybowski, N. Bansal, T.M. Duncan, NMR Spectroscopy of xenon in confined spaces: clathrates, intercalates, and zeolites, Annu. Rev. Phys. Chem. 42 (1991) 433–464;
P.J. Barrie, J. Klinowski, ^{129}Xe NMR as a probe for the study of microporous solids: a critical review, Progr. NMR Spectrosc. 24 (1992) 91–108;
M.A. Springuel-Huet, J.L. Bonardet, A. Gédéon, J. Fraissard, ^{129}Xe NMR for studying surface heterogeneity: well-known facts and new findings, Langmuir 13 (1997) 1229–1236;
M.A. Springuel-Huet, J.L. Bonardet, A. Gedeon, J. Fraissard, ^{129}Xe NMR overview of xenon physisorbed in porous solids, Magn. Reson. Chem. 37 (1999) S1–S13;
J.L. Bonardet, J. Fraissard, A. Gedeon, M.A. Springuel-Huet, Nuclear magnetic resonance of physisorbed ^{129}Xe used as a probe to investigate porous solids, Catal. Rev. 41 (1999) 115–225.

[3] A. Bifone, T. Pietrass, J. Kritzenberger, A. Pines, B.F. Chmelka, Surface study of supported metal particles by ^{129}Xe NMR, Phys. Rev. Lett. 74 (1995) 3277–3280.

[4] D. Raftery, H. Long, T. Meersmann, P.J. Grandinetti, L. Reven, A. Pines, High-field NMR of adsorbed xenon polarized by laser pumping, Phys. Rev. Lett. 66 (1991) 584–587;
T. Pietraß, A. Bifone, A. Pines, Adsorption properties of porous silicon characterized by optically enhanced ^{129}Xe NMR spectroscopy, Surf. Sci. Lett. 334 (1995) L730–L734;
Y.-Q. Song, H.C. Gaede, T. Pietraß, G.A. Barrall, G.C. Chingas, M.R. Ayers, A. Pines, Spin-polarized ^{129}Xe gas imaging of materials, J. Magn. Reson. A 115 (1995) 127–130.

[5] T.G. Walker, W. Happer, Spin-exchange optical pumping of noble-gas nuclei, Rev. Mod. Phys. 69 (1997) 629–642.

[6] U. Ruth, T. Hof, J. Schmidt, D. Fick, H.J. Jänsch, Production of nitrogen-free, hyperpolarized ^{129}Xe gas, Appl. Phys. B 68 (1999) 93–97.

[7] D. Stahl, H.J. Jänsch, An apparatus for NMR of laser-polarized ^{129}Xe on single crystal surfaces, Hyperfine Interact. 127 (2000) 469–474.

[8] L.W. Bruch, M.W. Cole, E. Zaremba, Physical Adsorption: Forces and Phenomena, The International Series of Monographs on Chemistry, Clarendon Press, Oxford, 1997.

[9] K. Watanabe, H. Kato, Y. Matsumoto, Photo-stimulated desorption of rare gas atoms induced by UV-NIR photons at a semiconductor surface, Surf. Sci. 446 (2000) L134–L139.

[10] E.G. Michel, P. Pervan, G.R. Castro, R. Miranda, K. Wandelt, Structural and electronic properties of K/Si(1 0 0)2×1, Phys. Rev. B 45 (1992) 11811–11822.

[11] B. Narloch, D. Menzel, Structural evidence for chemical contributions in the bonding of the heavy rare gases on a close-packed transition metal surface: Xe and Kr on Ru(0 0 1), Chem. Phys. Lett. 270 (1997) 163–168.

[12] H. Schlichting, Methoden und Mechanismen der thermischen Desorption: Adsorption-, Desorptions-Kinetik, Epitaxie und Ordnung von Edelgasschichten auf Ru(0 0 1). PhD thesis, Technische Universität, München, 1990.

[13] R.C. Weast (Ed.), CRC Handbook of Chemistry and Physics, 57 ed., CRC Press, Cleveland, OH, 1976.

[14] J. Xu, H.J. Jänsch, J.T. Yates Jr., Cryogenic trick for enhanced cooling using liquid nitrogen, J. Vac. Sci. Technol. A 11 (1993) 726–727.

[15] C.W. Leming, G.L. Pollack, Sublimation pressures of solid Ar, Kr, and Xe, Phys. Rev. B 2 (1970) 3323–3330.

[16] W.M. Yen, R.E. Norberg, Nuclear magnetic resonance of Xe^{129} in solid and liquid xenon, Phys. Rev. 131 (1963) 269–275.

[17] D.F. Cowgill, R.E. Norberg, Local-magnetic-field shift in natural xenon, Phys. Rev. B 6 (1972) 1636–1638.

[18] G.D. Cates, D.R. Benton, M. Gatzke, W. Happer, K.C. Hasson, N.R. Newbury, Laser production of large nuclear-spin polarization in frozen xenon, Phys. Rev. Lett. 65 (1990) 2591–2594.

[19] M. Gatzke, G.D. Cates, B. Driehuys, D. Fox, W. Happer, B. Saam, Extraordinarily slow nuclear spin relaxation in frozen laser-polarized ^{129}Xe, Phys. Rev. Lett. 70 (1993) 690–693.

[20] R.J. Fitzgerald, M. Gatzke, D.C. Fox, G.D. Cates, W. Happer, ^{129}Xe spin relaxation in frozen xenon, Phys. Rev. B 59 (1999) 8795–8811.

[21] A. Abragam, M. Goldman, Nuclear Magnetism: Order and Disorder, International Series of Monographs on Physics, Clarendon Press, Oxford, 1982.

[22] A. Abragam, The Principles of Nuclear Magnetism, Oxford University Press, Oxford, 1961.

[23] R.R. Ernst, G. Bodenhausen, A. Wokaun, Principles of Nuclear Magnetic Resonance in One and Two Dimensions, International Series of Monographs on Chemistry, vol. 14, Clarendon Press, Oxford, 1989.

[24] H.W. Long, H.C. Gaede, J. Shore, L. Reven, C.R. Bowers, J. Kritzenberger, T. Pietrass, A. Pines, P. Tang, J.A. Reimer, High-field cross polarization NMR from laser-polarized xenon to a polymer surface, J. Am. Chem. Soc. 115 (1993) 8491–8492.

[25] G. Neue, A ^{129}Xe-NMR study of Xe layers on graphon, Zeitschrift für Physikalische Chemie Neue Folge 152 (1987) 13–22.

[26] Y.Y. Tong, C. Rice, A. Wieckwski, E. Oldfield, A detailed NMR-based model for CO on Pt catalysts in an electrochemical environment: shifts, relaxation, back-bonding, and the Fermi-level density of states, J. Am. Chem. Soc. 122 (2000) 1123–1129.

[27] M. Detje, M. Röckelein, W. Preyß, H.D. Ebinger, H.J. Jänsch, H. Reich, R. Veith, W. Widdra, D. Fick, Adsorption of β-radioactive ^{8}Li on single crystal surfaces: TDS and NMR experiments, J. Vac. Sci. Technol. A 13 (1995) 2532;
W. Widdra, M. Detje, H.D. Ebinger, H.J. Jänsch, W. Preyß, H. Reich, R. Veith, D. Fick, M. Röckelein, H.-G. Völk, β-NMR on single-crystal surfaces: method, Rev. Sci. Instrum. 66 (1995) 2465–2475;
H. Arnolds, D. Fick, H. Unterhalt, A. Voß, H.J. Jänsch, Particle detected fourier transform NMR at single crystal surfaces—^{6}Li on Ru(0 0 1), Solid State Nucl. Magn. Reson. 11 (1998) 87–102;

H. Kleine, D. Fick, Electric-field gradients from NMR measurements on the Si(1 1 1)3 × 1-Li reconstruction, New J. Phys. 3 (2001) 1.1–1.11.

[28] G. Kirchner, M. Czanta, G. Dellemann, H.J. Jänsch, W. Mannstadt, J.J. Paggel, R. Platzer, C. Weindel, H. Winnefeld, D. Fick, Coverage dependent local density of states at Li-atoms adsorbed on a Ru(0 0 1)-surface, Surf. Sci. 494 (2001) 281–288.

[29] H.D. Ebinger, H. Arnolds, C. Polenz, B. Polivka, W. Preyß, R. Veith, D. Fick, H.J. Jänsch, Adsorption and diffusion of Li on a Ru(0 0 1) surface: an NMR study, Surf. Sci. 412/413 (1998) 586–615.

[30] R. Gomer, Diffusion of adsorbates on metal surfaces, Rep. Prog. Phys. 53 (1990) 917.

[31] B. Poelsema, L.K. Verheij, G. Comsa, Adsorption, 2D phase transition and commensurate 2D phase of Xe on Pt(1 1 1), Surf. Sci. 152/153 (1985) 851–858.

[32] D.L. Meixner, S.M. George, Surface diffusion of xenon on Pt(1 1 1), J. Chem. Phys. 98 (1993) 9115–9125.

[33] J.P. Korb, M. Winterhalter, H.M. McConnell, Theory of spin relaxation by translational diffusion in two-dimensional systems, J. Chem. Phys. 80 (1984) 1059–1068.

[34] E. Wimmer, H. Krakauer, M. Weinert, A.J. Freeman, Full-potential self-consistent linearized-augmented-plane-wave method for calculating the electronic structure of molecules and surfaces: O_2 molecule, Phys. Rev. B 24 (1981) 864–875;
M. Weinert, E. Wimmer, A.J. Freeman, Total-energy all-electron density functional method for bulk solids and surfaces, Phys. Rev. B 26 (1982) 4571–4578;
H.J.F. Jansen, A.J. Freeman, Total-energy full-potential linearized augmented-plane-wave method for bulk solids: electronic and structural properties of tungsten, Phys. Rev. B 30 (1984) 561–569.

[35] A. Canning, W. Mannstadt, A.J. Freeman, Parallelization of the FLAPW method, Comput. Phys. Commun. 130 (2000) 233–243.

[36] W. Mannstadt, A.J. Freeman, LDA theory of the coverage dependence of the local density of states: Li adsorbed on Ru(0 0 1), Phys. Rev. B 57 (1998) 13289.

[37] H.J. Jänsch, H. Arnolds, H.D. Ebinger, C. Polenz, B. Polivka, G.J. Pietsch, W. Preyß, V. Saier, R. Veith, D. Fick, Coverage dependence of the local density of states at the Fermi energy—Li adsorbed on Ru(0 0 1), Phys. Rev. Lett. 75 (1995) 120–123.

[38] D.M. Eigler, P.S. Weiss, E.K. Schweizer, N.D. Lang, Imaging Xe with a low-temperature scanning tunneling microscope, Phys. Rev. Lett. 66 (1991) 1189–1192.

[39] K. Wandelt, B. Gumhalter, Face specifity of the Xe/Pd bond and the s-resonance model, Surf. Sci. 140 (1984) 355–376.

[40] H.J. Jänsch, T. Hof, U. Ruth, J. Schmidt, D. Stahl, D. Fick, NMR of surfaces: sub-monolayer sensitivity with hyperpolarized ^{129}Xe, Chem. Phys. Lett. 296 (1998) 146–150.